PAPER

Re-Du-Ning inhalation solution exerts suppressive effect on the secretion of inflammatory mediators *via* inhibiting IKKα/β/IκBα/NF-κB, MAPKs/AP-1, and TBK1/IRF3 signaling pathways in lipopolysaccharide stimulated RAW 264.7 macrophages

Yi Zhang,[a] Brian Chi-Yan Cheng,[bc] Ran Xie,[d] Bing Xu,[a] Xiao Yan Gao[a] and Gan Luo ID *[a]

Background: *Re-Du-Ning* inhalation solution (RIS) is a novel preparation derived from the *Re-Du-Ning* injection, which has been clinically used to treat respiratory diseases such as pneumonia for more than twenty years in China. However, scant reports have been issued on its anti-inflammatory mechanisms. *Aim*: we investigated the suppressive effect of RIS on inflammatory mediators and explored the underlying mechanism of action. *Methods*: RIS freeze dried powder was characterized by HPLC analysis. Lipopolysaccharide (LPS)-stimulated RAW 264.7 macrophage was selected as the cell model. The cell viability was determined by using the MTT assay. Moreover, the production of nitric oxide (NO) was measured by the Griess reaction. The protein secretions from inflammatory mediators were determined by the enzyme-linked immunosorbent assay (ELISA). The protein levels and enzyme activities were examined by Western blotting. The nuclear translocation of nuclear factor-kappa B (NF-κB), AP-1, and IRF3 was further explored by immunofluorescence assay. *Results*: the viability of the RAW 264.7 cells was not significantly changed after 24 h incubation with RIS concentration up to 400 μg mL^{-1}. The RIS remarkably reduced the production of NO and prostaglandin E$_2$ (PGE$_2$), and downregulated the expression of iNOS and COX-2. The concentrations of cytokines (IL-1β, IL-6, and TNF-α) and chemokines (MCP-1, CCL-5, and MIP-1α) in the culture medium were significantly decreased by the RIS treatment. Furthermore, the phosphorylation of IκB-α, IKKα/β, TBK1, ERK, p38, JNK, NF-κB, AP-1, and IRF3 was downregulated by the RIS treatment. The nuclear translocation of NF-κB, AP-1, and IRF3 was also inhibited after the RIS treatment. *Conclusion*: the suppressive effect of RIS is associated with the regulated NF-κB, AP-1, and IRF3 and their upstream proteins. This study provides a pharmacological basis for the application of RIS in the treatment of inflammatory disorders.

Introduction

Inflammatory responses play an important role in immune homeostasis and are essential for host survival.[1] However, hyperactive and chronic inflammation represents a central driving force in many disorders such as asthma,[2] pneumonia,[3] rheumatoid arthritis,[4] and chronic obstructive pulmonary disease.[5] These diseases impose a huge burden on the society in terms of incurred disability and premature mortality.[6–8] Multiple innate immune cells contribute to the pathophysiological processes of inflammatory diseases, with macrophages playing a significant role.[9] Lipopolysaccharide (LPS) is a pathogenic endotoxin present in the outer membrane of Gram-negative bacteria, which can activate the toll-like receptor (TLR)-4 and the downstream signaling pathways including IKKα/β/IκBα/NF-κB, MAPKs/AP-1, and TBK1/IRF3.[10] This in turn activates an inflammatory cascade with the production of inflammation-related molecules such as nitric oxide (NO), interleukin-6 (IL-6), and tumour necrosis factor (TNF-α), providing a positive feed-back to the TLR4 signaling pathways, which results in persistent inflammation and favours the induction of autoimmunity.[11–13] Therefore, targeting the TLR4 signaling is one of the focuses in developing effective anti-inflammatory agents for acute and chronic inflammatory diseases.[14]

Traditional Chinese Medicine (TCM) treatment has been recently applied to offer a different approach to prevent or cure inflammatory diseases.[15] The *Re-Du-Ning* inhalation solution (RIS) is a novel preparation derived from the *Re-Du-Ning* injection

[a]*School of Chinese Materia Medica, Beijing University of Chinese Medicine, Beijing 100102, China. E-mail: luna049@126.com*

[b]*College of Professional and Continuing Education, Hong Kong Polytechnic University, Hong Kong 999077, China*

[c]*Quality Healthcare Medical Services, Hong Kong 999077, China*

[d]*Institute of Chinese Materia Medica, China Academy of Chinese Medical Science, Beijing 100700, China*

(RDNI). The RDNI has been clinically used as an aerosol to treat respiratory diseases such as pneumonia for more than twenty years in the People's Republic of China.[16] This preparation is composed of the flowers of *Lonicera japonica*, the fruits of *Gardenia jasminoides*, and the dried aerial parts of *Artemisia apiacea* in the ratio of 25 : 15 : 12.[17] It has been reported that these herbs are of low toxicity and have been used in China for hundreds of years to treat early febrile diseases, exogenous fever, and boils.[18–21] Previous studies have showed that the main compounds in the flowers of *Lonicera japonica* (*e.g.* chlorogenic acid),[22,23] the fruits of *Gardenia jasminoides* (*e.g.* geniposide)[10,24] and *Artemisia apiacea* (*e.g.* artemisinin)[25] have strong anti-inflammatory activities *via* inhibition of the TLR4 signaling pathway. However, as a new aerosol preparation, there are no reports in the literature about the pharmacological properties of RIS. In order to provide pharmacological justification for the use of RIS as an anti-inflammatory agent, we employed a classic inflammatory cell model called the LPS-stimulated RAW 264.7 macrophages, to investigate the suppressive effect of RIS on inflammatory mediators and to explore the underling mechanisms.

Materials

Modified Griess reagent, 3-[4,5-dimethylthiazol-2-yl]-2,5-diphenyl tetrazolium bromide (MTT), lipopolysaccharide (LPS, *Escherichia coli* O55:B5), and bovine serum albumin were bought from Sigma Chemical Co. (St. Louis MO, USA). Penicillin-streptomycin solution was obtained from Caisson labs (Smithfield, UT, USA). Dulbecco's Modified Eagle Medium (DMEM) was acquired from Corning Cellgro (Manassas, VA, USA). Fetal bovine serum (FBS) was purchased from Biological Industries Co. (Beth-Haemek, Israel). Tumor necrosis factor α (TNF-α), interleukin-6 (IL-6), interleukin 1β (IL-1β), macrophage inflammatory protein (MIP)-1α, monocyte chemoattractant protein (MCP)-1, and chemokine (C–C motif) ligand 5 (CCL-5) ELISA kits were purchased from Thermo Fisher Scientific (San Diego, CA). Prostaglandin E2 (PGE2) ELISA kit was provided by Enzo Life Sciences (Exeter, UK). IκB kinase α (IKKα) and sp1 monoclonal antibodies were supplied by Santa Cruz Biotechnology (Santa Cruz, CA, USA). Interferon regulatory factor 3 (IRF3) was purchased from Abcam (Cambridge, UK). Phospho-NF-κB p65 (Ser536), NF-κB p65, phospho-c-Jun (Ser73), c-Jun, cyclooxygenase-2 (COX-2), inducible nitric oxide synthase (iNOS), phospho-IRF3 (Ser396), phospho-IκBα (Ser32), IκBα, phospho-IKKα/β (Ser176/180), phospho-ERK (Thr202/Tyr204), extracellular signal-regulated kinase (ERK), phospho-JNK (Thr183/Tyr185), c-Jun N-terminal kinase (JNK), phospho-p38 (Thr180/Tyr182), p38 mitogen-activated protein kinase (p38), TANK-binding kinase 1 (TBK1), phospho-TBK1 (Ser172), anti-rabbit IgG HRP linked anti-body, and Alexa Fluor 488-conjugated secondary antibody were bought from Cell Signaling Technology (Boston, MA, USA).

Methods

Preparation of RIS powder

RIS (batch number: 170803) was provided by Jiangsu Kanion Pharmaceutical Corporation (Jiangsu, China). RIS (200 mL) was concentrated by rotary evaporation under reduced pressure to remove the solvent. The concentrated extracts were rapidly frozen at −80 °C, and then dried in a freeze-dryer (FD-1D-80, Biocool, Beijing, China). The yield of the powdered RIS was 3.87%. To characterize the RIS powder, 0.3542 g of the RIS powder was dissolved with 50% ethanol and diluted to 25 mL. Then, the diluent was filtered through a 0.45 μm Millipore membrane filter for HPLC analysis. To prepare the sample solution for bioassays, RIS was freshly dissolved in DMSO, and then diluted with cell culture medium to various concentrations.

Content determination of RIS powder

For the quality control of the prepared RIS, HPLC analysis was performed using an LC-20a HPLC system (Shimadzu Corporation, Tokyo, Japan) consisting of a vacuum degasser, a quaternary pump, an auto sampler, a thermostatic column compartment, and a diode array detector. The separation was conducted on the Agilent Zorbax SB C18 column (250 mm × 4.6 mm with 5 μm particle size) with a gradient mobile phase of solvent A (methanol) and solvent B (0.1% phosphoric acid in water). The HPLC elution profile was as follows: 0–10 min, 15–25% A; 10–30 min, 25–35% A; 30–60 min, 35–50% A. The flow rate was maintained at 0.8 mL min^{-1} and the column temperature was set at 30 °C. The chromatograms were monitored with the DAD detector at wavelengths of 237 nm and 324 nm to detect geniposide and chlorogenic acid, respectively. Each sample of 10 μL volume was injected for analysis.

HPLC fingerprint analysis of RIS

In order to obtain comprehensive chemical information of the RIS powder, fingerprint analysis was carried out using a liquid chromatography with the Agilent 1260 LC system (Agilent Technologies, California, USA) equipped with a quaternary pump, autosampler injector, and a DAD detector adjusted to 225 nm. The chromatographic separation was performed on a Phenomenex Luna C18 column (4.6 × 150 mm, 5 μm; Phenomenex, Los Angeles, USA) at room temperature. The mobile phase constituted of A (methanol) and B (0.1% phosphoric acid). The gradient elution program was as follows: 0–50 min, 20–60% A; 50–60 min, 60% A. The flow rate was set at 0.8 mL min^{-1}. Each sample of 5 μL volume was injected for analysis.

Cell culture

The RAW 264.7 murine macrophage cell line was obtained from American Type Culture Collection (Manassa, VA, USA). Cells were incubated in the DMEM medium at 37 °C with 5% CO$_2$. The penicillin/streptomycin antibiotics (1%) and heat-inactivated FBS (10%) were added into the DMEM medium. For each experiment, the cells were seeded in plates and allowed to attach for 24 h. Next, the fresh medium supplemented with RIS or the vehicle was substituted in the culture medium.

Cell viability assay

The effect of RIS on the RAW 264.7 cells' viability was measured by the MTT assay. Briefly, 6 × 10^3 cells (100 μL) per well were

seeded in 96 well plates and allowed to adhere overnight. Various concentrations of RIS (12.5–400 μg mL^{-1}) were added into the cells, incubated for 1 h, and then treated in the presence or absence of LPS (1 μg mL^{-1}) for another 24 h. Subsequently, 10 μL of the MTT solution (5 mg mL^{-1}) was added in each well and incubated for 3 h at 37 °C. The supernatant was then removed and the remaining formazan crystals were dissolved with 100 μL of DMSO in each well. The absorbance at 570 nm was determined using a microplate spectrophotometer (BMG SPECTROstar Nano, Germany). The value of cell viability in the control group was set as 100%. Six replicate wells were used.

Determination of nitric oxide (NO) production

NO production was assayed by measuring nitrite (a stable degradation product of NO) in the supernatants of cultured RAW 264.7 cells using the Griess modified reagent. Briefly, 2 × 10^5 cells per well were seeded in 24 well plates. The volume of cell inoculation was 1 mL. After 24 h incubation, the cells were pre-treated with RIS for 1 h, followed by 1 μg mL^{-1} of LPS, and then incubated in a humidified incubator at 37 °C for 24 h. 100 μL of the supernatant was collected, mixed with an equal volume of Griess reagent, and incubated for 10 min at room temperature. The absorbance measured at 540 nm was used as an indication of the nitrite concentration. Sodium nitrite (NaNO$_2$) was used to produce a standard curve of nitrite concentrations. Four replicate wells were used.

Enzyme-linked immunosorbent assay (ELISA)

To measure the production of MIP-1α, MCP-1, TNF-α, IL-6, IL-1β, MCP-1, CCL-5, and PGE$_2$, the cells were incubated with different concentrations of RIS in either the presence or absence of LPS for 24 h. 100 μL of the culture medium supernatant was collected and the concentrations of pro-inflammatory cytokines and chemokines in the cell culture medium were calculated, based on the concentrations of the standard solution, using ELISA kits according to the manufacturer's instructions. Four replicate wells were used.

Cytoplasmic and nuclear proteins' extraction

Cytoplasmic and nuclear proteins were extracted using the nuclear extraction kit (Solarbio, Beijing, China) according to the manufacturer's instructions. Briefly, the RAW 264.7 cells were seeded in 100 mm diameter culture dishes (1 × 10^6 cells, 10 mL), incubated for 24 h, and then treated with 100 and 200 μg mL^{-1} of RIS for 1 h. LPS (1 μg mL^{-1}) was then added into the culture medium and incubated at 37 °C for 60 min. The cells were harvested and washed with PBS. The ice-cold cytoplasmic protein extraction solution was added to separate the cyto-plasmic and nuclear proteins after centrifugation. The same was then added to the nuclear fraction for protein extraction. Three replicates were used.

Western blot analysis

Western blot was performed to explore the underlying mecha-nism of anti-inflammatory action of RIS. Briefly, the RAW 264.7

cells were seeded in 60 mm culture dishes (4 × 10^5 cells, 3 mL) and treated with 100 and 200 μg mL^{-1} of RIS for 1 h. LPS (1 μg mL^{-1}) was then added into the culture medium and incubated at 37 °C for 30 min or 60 min. The cells were washed with cold PBS, and then lysed with cold Radio Immunoprecipitation Assay (RIPA) protein extraction buffer containing 1% protease and phosphatase inhibitors (Beyotime Biotechnology, Beijing, China) for 30 min on ice. An aliquot of 20 μg of the supernatant protein from each of the samples was heated with 4 × sodium dodecyl sulfate (SDS) sample buffer at 95 °C for 8 min, and separated electrophoretically on a 10% SDS-polyacrylamide gel. Subsequently, the proteins were transferred onto 0.45 μm pore size PMSF membranes for 3 h and blocked for 1 h. The PMSF membranes were then exposed to indicate the primary anti-bodies in the blocking buffer at 1 : 500 or 1 : 1000 dilutions overnight at 4 °C. The membranes were then incubated with the anti-rabbit IgG secondary antibody conjugated with horseradish at 1 : 2000 dilutions for 1 h. The visualization was performed using Tanon 5200 Multi chemiluminescent imaging system (Tanon Science & Technology Co., Ltd., Shanghai, China) with enhanced-chemiluminescence substrate, and the blots were analyzed using the Image J software (National Institutes of Health [NIH], Bethesda, MD, USA). The protein levels were corrected with the values determined from the β-actin blots. Three replicates were used.

Immunofluorescence staining

Immunofluorescence staining was conducted to detect the NF-κB/p65, AP-1/c-Jun, and IRF3 localization after the RIS treatment. Briefly, with an inoculation volume of 1 mL, 1 × 10^4 cells were cultured on coverslips (Cat. 177399; Thermo Fisher Scientific) overnight, treated with RIS (200 μg mL^{-1}), and then fixed with formaldehyde in PBS (w/v, 4%) for 15 min. Then, the cells were washed with PBS and permeabilized with Triton X-100 (0.25%) in 30 min at 37 °C and blocked for 1 h with BSA (2%). The cells were then incubated with NF-κB/p65 (1 : 300), c-Jun (1 : 300), and IRF3 (1 : 100) overnight at 4 °C, respectively. After washing with cold PBS, the cells were incubated with Alexa Fluor 488-conjugated secondary antibody (1 : 500) for 1 h at room temperature. The coverslips were mounted using Fluoroshield with DAPI (YESEN, Shanghai, China) and visualized using the Nikon A1R Eclipse Ti confocal microscope (Nikon Corp., Tokyo, Japan).

Statistical analysis

All values were given as the mean ± standard deviation with at least three replicates for each assay. The statistical differences were determined using one-way ANOVA followed by Turkey's multiple comparisons test. When the value of p was below 0.05, the average values of the different groups were considered significantly different.

Results

Characterization of RIS powder

In this study, the HPLC chromatogram showed that geniposide and chlorogenic acid were present in the RIS powder (see Fig. 1).
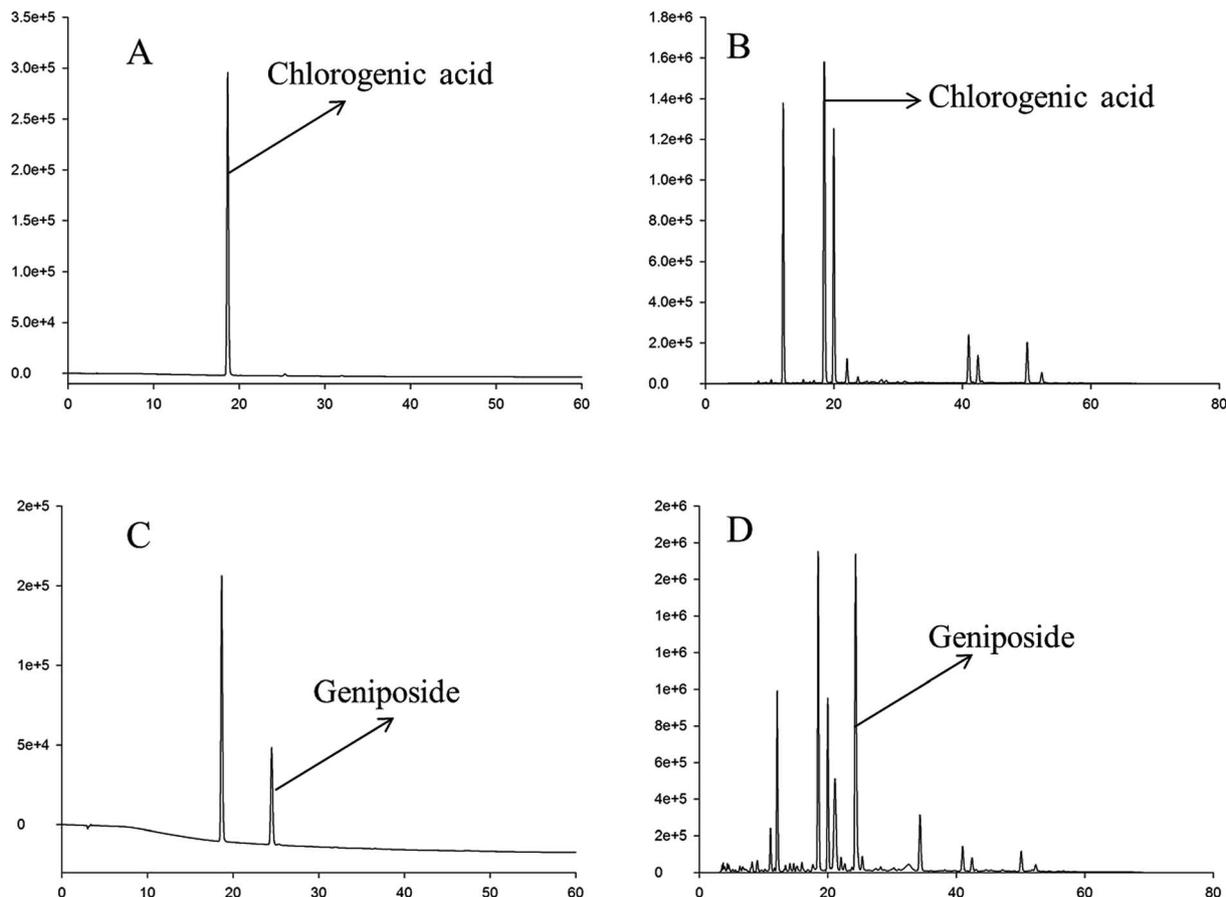
Fig. 1 HPLC chromatograms of chlorogenic acid, geniposide, and RIS at different wavelengths. (A) HPLC chromatogram of chlorogenic acid at 324 nm. (B) HPLC chromatogram of geniposide at 237 nm. (C) HPLC chromatogram of the RIS sample at 324 nm. (D) HPLC chromatogram of the RIS sample at 237 nm.

The mean contents of chlorogenic acid and geniposide in the RIS powder were 70.03 and 120.50 mg g^{-1}, respectively.

HPLC fingerprint analysis of RIS

In the HPLC fingerprint analysis of RIS, geniposide was selected as the reference substance. As is shown in Fig. 2, peak S was geniposide. Except geniposid, other 13 common peaks were confirmed. Table 1 shows the relative retention times and peak area ratios of 13 common peaks and geniposide. Relative retention time means the ratio of the retention time of a common peak to geniposide. Similarly, the peak area ratio is the ratio of the peak area of a common peak to geniposide.

Effect of RIS on cell viability

To determine the sub-cytotoxic concentrations of RIS, the MTT assay was conducted. As shown in Fig. 3, the viability of the RAW 264.7 cells was not significantly changed ($p > 0.05$) up to 400 µg mL^{-1} concentration of RIS after 24 h incubation with LPS of 1 µg mL^{-1}. Therefore, we chose the concentrations of RIS as 25, 50, 100, and 200 µg mL^{-1} in the following experiments.

Effect of RIS on the production of NO and PGE2 and the expression of iNOS and COX-2

Next, we determined the inflammatory mediators including NO and PGE2 inhibitory activity by RIS in LPS-stimulated RAW 264.7 macrophages. As shown in Fig. 4A and B, the production of NO and PGE$_2$ was strongly inhibited by RIS in a concentration-dependent manner up to 33% and 70%, respectively, in the RAW 264.7 cells ($p < 0.01$). Furthermore, we detected the expression of key enzymes responsible for the NO and PGE$_2$ production including iNOS and COX-2. The LPS-stimulated RAW 264.7 cells strongly upregulated the protein levels of iNOS and COX-2, whereas this effect was notably ($p < 0.01$) blocked by RIS (100 and 200 µg mL^{-1}) in a concentration-dependent manner (Fig. 4C and E).

Effect of RIS on the production of pro-inflammatory cytokines and chemokines

It has been reported that LPS activates the TLR4 signaling pathway and subsequently produces pro-inflammatory cytokines and chemokines in the macrophage cells.[15,26,27] In line with the previous studies, we observed that LPS remarkably promoted the release of pro-inflammatory cytokines (see
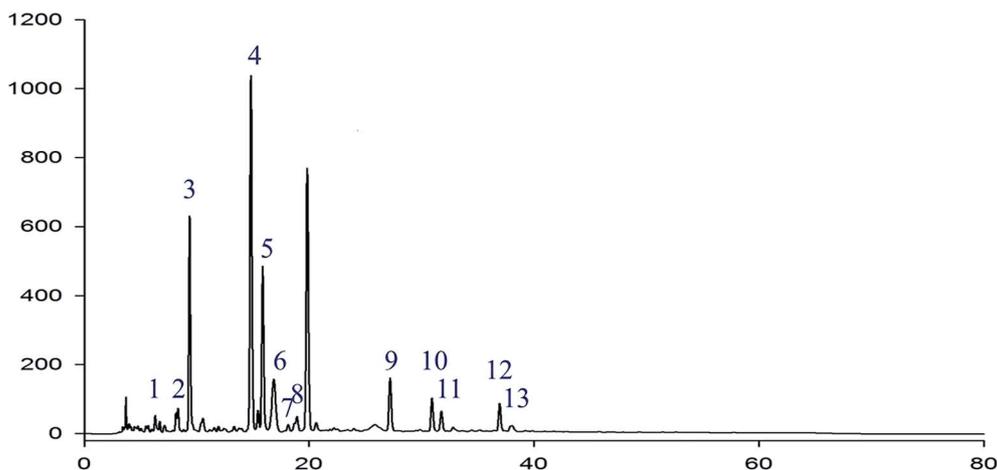
Fig. 2 HPLC fingerprint chromatogram of RIS Peak S is geniposide. Except geniposide, other 13 common peaks were detected at 225 nm.

Table 1 Relative retention times and peak area ratios of 13 common peaks and geniposide

Peak no.	Relative retention time	Peak area ratio
1	0.286	0.03
2	0.400	0.05
3	0.462	0.62
4	0.759	1.28
5	0.810	0.48
6	0.835	0.11
7	0.912	0.01
8	0.956	0.03
S	1.000	1.00
9	1.374	0.10
10	1.613	0.08
11	1.639	0.05
12	1.934	0.08
13	1.957	0.01

Fig. 5A–C) such as IL-1β, IL-6, and TNF-α as compared with the control cells. RIS efficiently suppressed the elevated cytokine levels in LPS-treated macrophages in a concentration-dependent manner. Moreover, as shown in Fig. 5D–F, the production of chemokines including MIP-1α, CCL-5, and MCP-1 was significantly elevated after the LPS treatment ($p < 0.01$), indicating that RIS decreased the LPS-induced production of these chemokines ($p < 0.05$ or $p < 0.01$) in an effective and concentration-dependent manner.

Effect of RIS on the nuclear translocation of NF-κB, AP-1, and IRF3 in RAW 264.7 cells

Following LPS stimulation, NF-κB, AP-1, and IRF3 are activated by post-translational modifications, and translocate into the nucleus to induce the transcription of the pro-inflammatory cytokines and chemokines.[28,29] Therefore, we firstly investigated the nuclear translocation of these three transcription factors by Western blot analysis. As shown in Fig. 6, the nuclear protein levels of NF-κB/p65, AP-1/c-Jun, and IRF3 were

significantly up-regulated after the LPS stimulation, and the RIS treatment markedly reduced the nuclear accumulation of NF-κB/p65, AP-1/c-Jun, and IRF3. The cytoplasmic proteins of these transcriptional factors were not significantly changed after the RIS treatment.

Next, we performed an immunofluorescence assay to examine the nuclear localization of NF-κB/p65, AP-1/c-Jun, and IRF3. We observed that NF-κB/p65, AP-1/c-Jun, and IRF3 were translocated from the cytoplasm to the nucleus after the LPS treatment, whereas RIS prevented the LPS-induced nuclear translocation in the RAW 264.7 cells (Fig. 7).

Effect of RIS on the IKKα/β/IκBα/NF-κB, MAPKs/AP-1, and TBK1/IRF3 signaling pathways

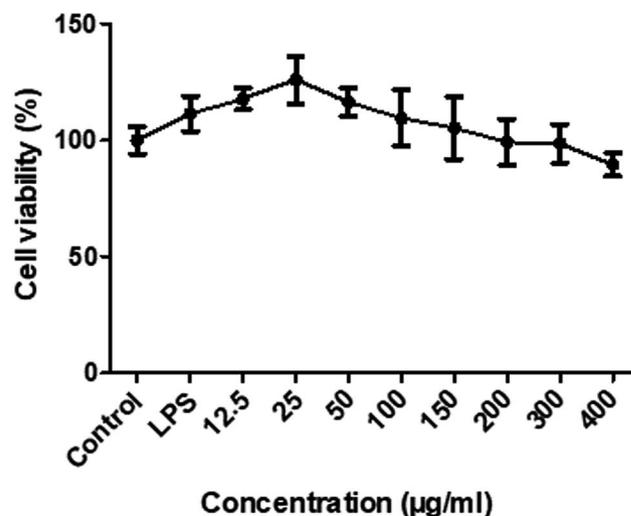LPS binds to TLR4 and leads to the activation of NF-κB, AP-1, and IRF3 through the recruitment and activation of the

Fig. 3 RIS does not affect cell growth in RAW 264.7 macrophages cells were treated with various concentrations of RIS (12.5–400 µg mL^{-1}) for 24 h. The total number of viable cells was determined by the MTT assay. Values are mean ± SEM of six independent observations.
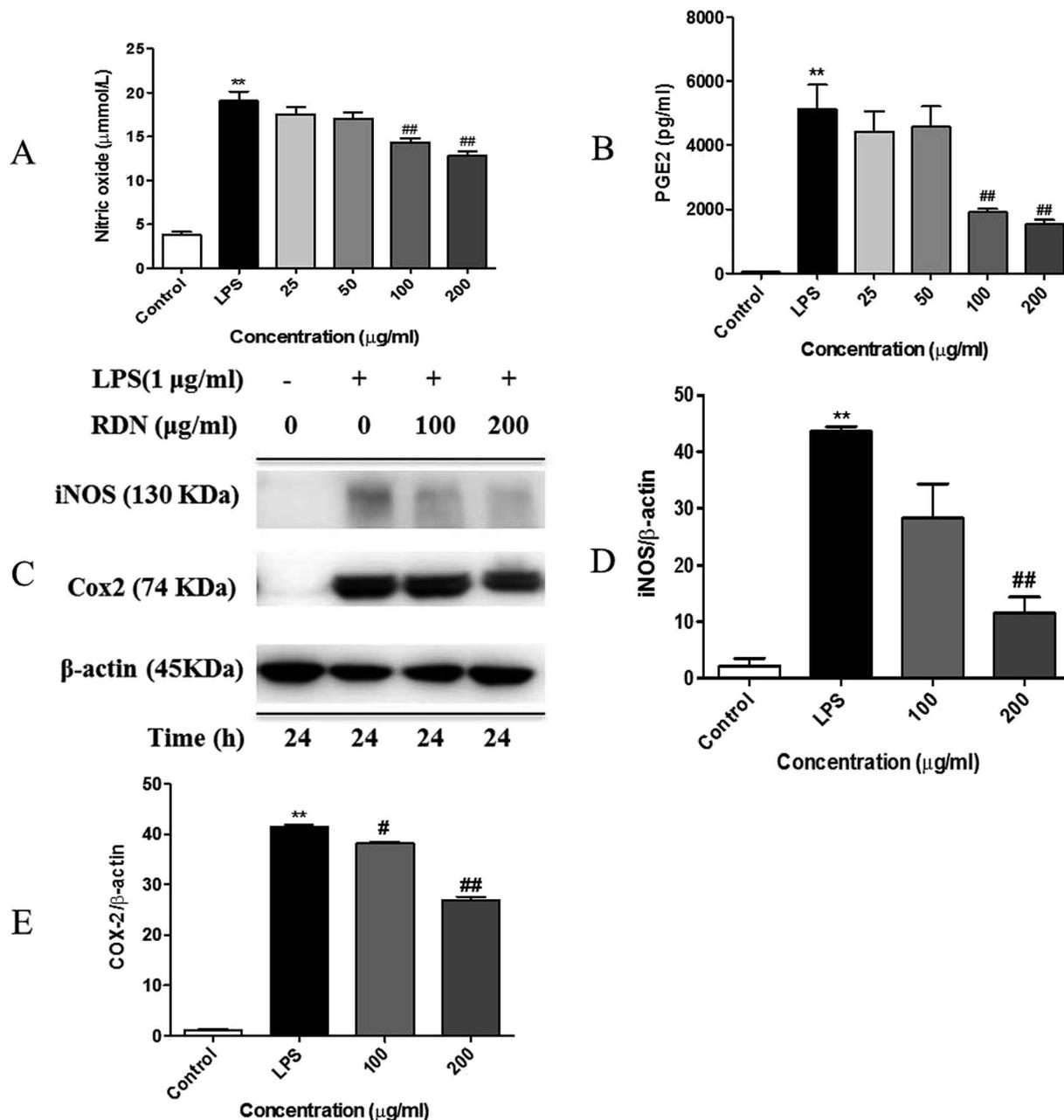
Fig. 4 RIS inhibits the production of NO and PGE_2 and the expression of iNOS and COX-2 in the LPS activated RAW 264.7 macrophages cells were incubated with indicated concentrations of RIS for 24 h with or without LPS. (A) Levels of NO in the culture supernatants of RAW 264.7 cells activated with LPS (1 μg mL^{-1}) in the presence or absence of RIS were determined by the Griess assay. (B) Levels of PGE_2 in the culture supernatants of RAW 264.7 cells treated with LPS (1 μg mL^{-1}) in the presence or absence of RIS were analyzed by ELISA. (C−E) The expression levels of iNOS, COX-2, and β-actin were analyzed by immunoblotting using whole cell lysates. The data shown are the mean ± SEM of three experiments. **$p < 0.01$ is significantly different from the control. #$p < 0.05$ and ##$p < 0.01$ are different from the LPS alone.

upstream proteins.[24,27] Therefore, we examined the expression of molecular components of TLR4 related pathways in the RAW 264.7 cells. As shown in Fig. 7 and 8, the phosphorylation levels of IKKα/β and IκBα were significantly up-regulated by the LPS treatment. RIS markedly decreased the LPS-induced elevation of the phosphorylated IKKα/β and IκBα in a concentration-dependent manner. Moreover, the phosphorylation of NF-κB subunit p65 was significantly increased after the LPS treatment, whereas RIS strongly exerted the down-regulative effect on the phosphorylated p65, suggesting that RIS inhibited the IKKα/β/IκBα/NF-κB signaling pathway. Furthermore, the phosphorylation levels of MAPKs including p38, ERK, and JNK were significantly increased after the LPS stimulation in the RAW 264.7 cells. However, RIS dramatically inhibited the LPS-induced upregulation of these three key protein kinases in a concentration-dependent manner. RIS also reduced the phosphorylation level of the down-stream protein of MAPKs
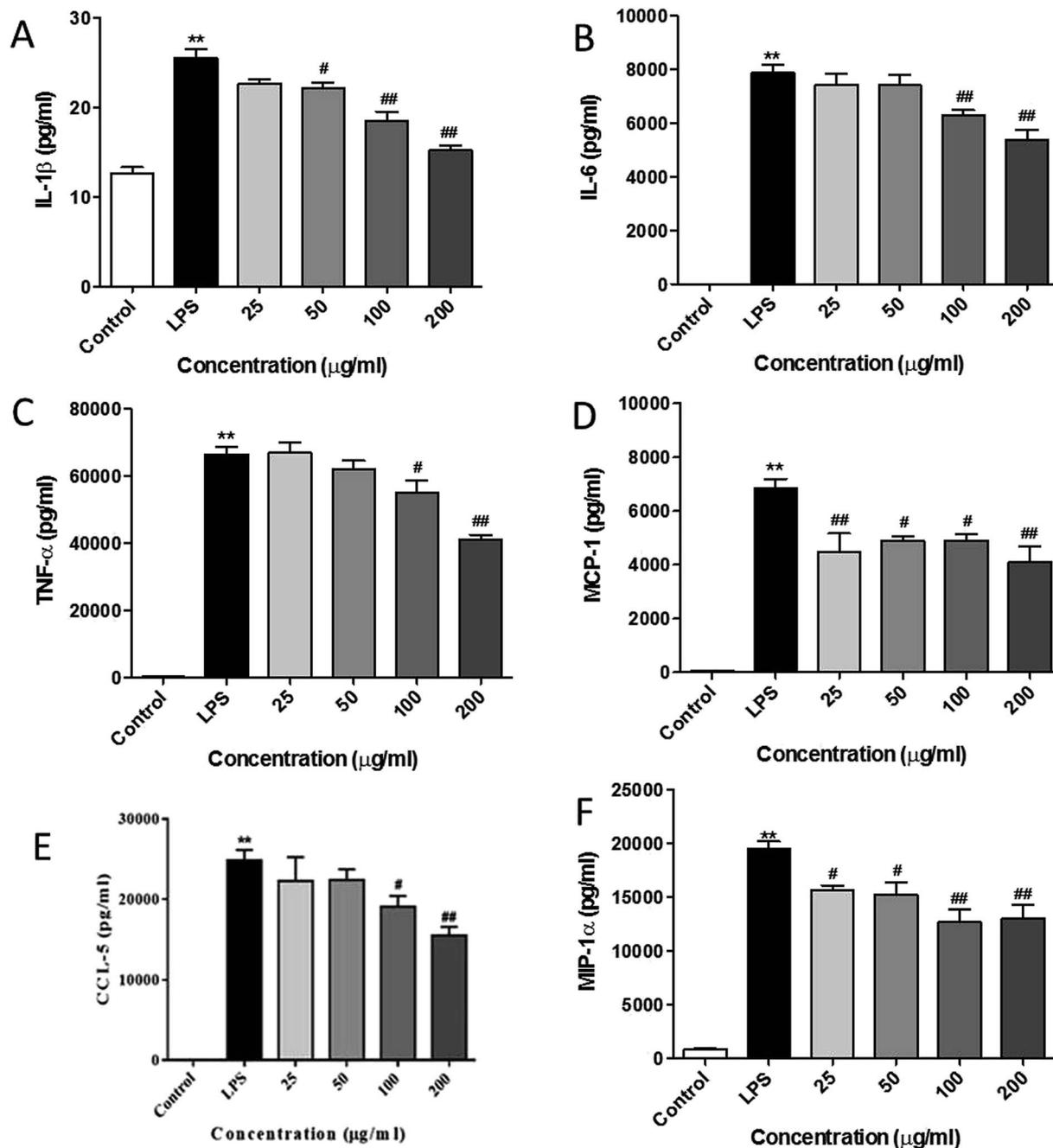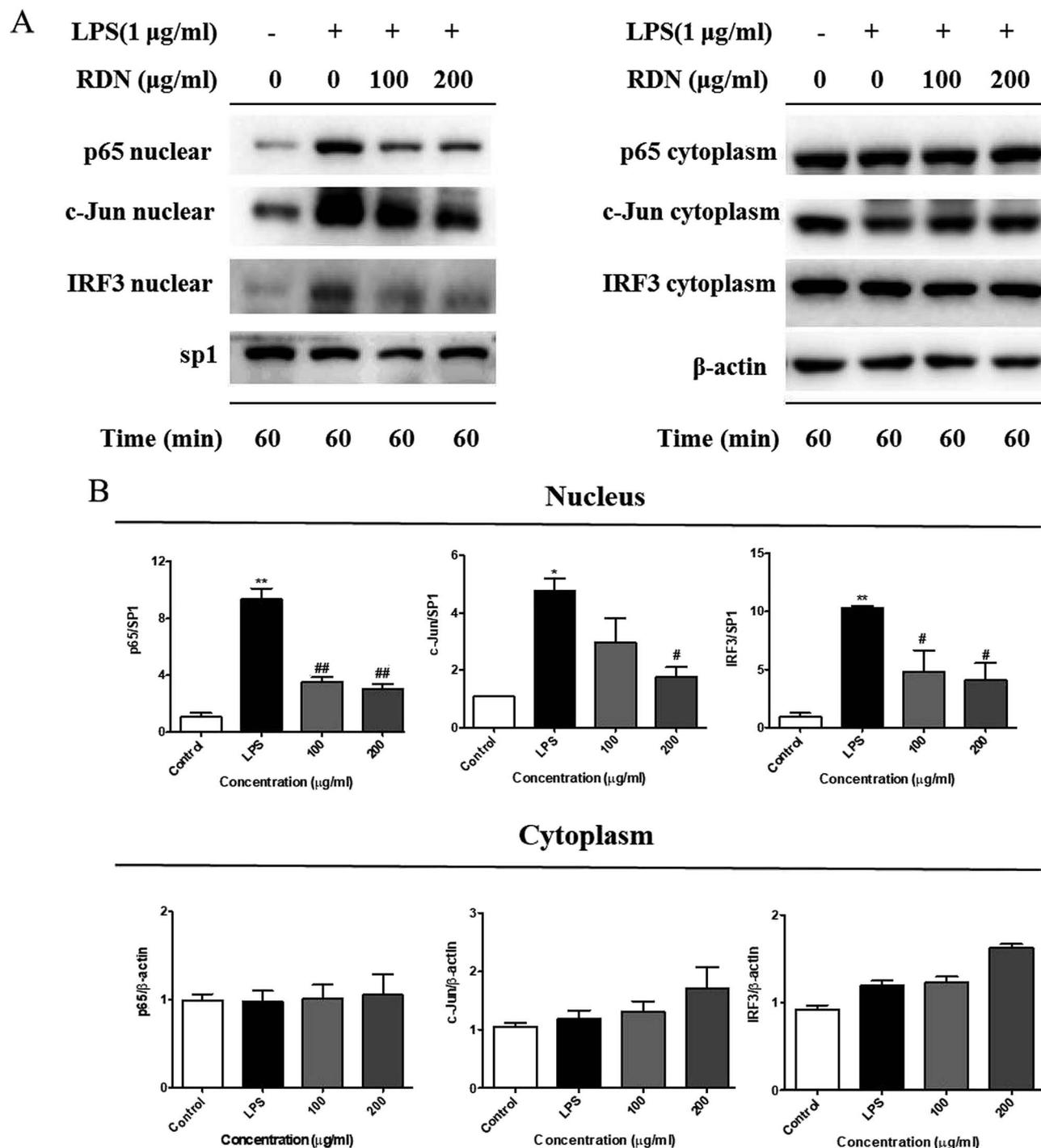
Fig. 5 RIS inhibits the production of pro-inflammatory cytokines and chemokines in the LPS activated RAW 264.7 macrophages cells were incubated with indicated concentrations of RIS for 1 h and then stimulated with LPS for 24 h. The cell-free supernatants were collected to detect (A) IL-1β; (B) IL-6; (C) TNF-α; (D) MCP-1; (E) CCL-5; (F) MIP-1α concentrations via ELISA after the LPS treatment for 24 h. The data shown are the mean ± SEM of four experiments. $**p < 0.01$ is significantly different from the control. $^{#}p < 0.05$ and $^{##}p < 0.01$ are different from the LPS alone.

such as the AP-1 subunit c-Jun, indicating that it has a potential inhibitory effect on the MAPKs/AP-1 signaling. In addition, we also observed that RIS notably blocked the LPS-induced, upregulated protein expression of phosphorylated TBK1. The phosphorylation level of IRF3 and the downstream protein of TBK1 were also strongly suppressed by the RIS treatment after LPS activation, suggesting that the TBK1/IRF3 signaling pathway was also modulated by RIS (Fig. 8 and 9).

Discussion

The anti-inflammatory effects and mechanisms of RDNI have been previously reported.[30] In this study, RDNI showed significant suppressive effect on the production of inflammatory mediators in the concentration range of 810–6500 μg mL^{-1} in the LPS-stimulated RAW 264.7 cells.[30] However, RIS exhibited an effective inhibitory effect on the secretion of inflammatory

Fig. 6   RIS inhibits the nuclear protein levels of NF-κB/p65, AP-1/c-Jun, and IRF3 in the LPS activated RAW 264.7 macrophages cells were incubated with indicated concentrations of RIS for 1 h and then stimulated with LPS for 1 h. (A) The nuclear and cytoplasmic protein levels of NF-κB/p65, AP-1/c-Jun, and IRF3 were determined by Western-blotting. (B) The bar graphs show protein levels of NF-κB/p65, AP-1/c-Jun, and IRF3. Values are the mean ± SEM of four experiments. **$p < 0.01$ is significantly different from the control. #$p < 0.05$ and ##$p < 0.01$ are different from the LPS alone.

mediators in RAW 264.7 cells in the concentration range of 100–200 μg mL⁻¹. Thus, it could be concluded that RIS had a better anti-inflammatory performance than RDNI.

Moreover, we did some exploratory work more deeply and comprehensively based on the former research.[30] The nuclear translocation of NF-κB, AP-1, and IRF3 were all studied. The effects of RIS on the three signalling pathways of TLR4 (IKKα/β/ IκBα/NF-κB, MAPKs/AP-1, and TBK1/IRF3) in the LPS induced RAW 264.7 cells were investigated in our study as well.

In the present study, chlorogenic acid and geniposide were identified in freeze dried RIS powder using HPLC analysis. It has been reported that chlorogenic acid inhibits the production of cytokines such as IL-1β, TNF-a, and IL-6 in the LPS-stimulated RAW 264.7 cells.[31] It also suppressed the
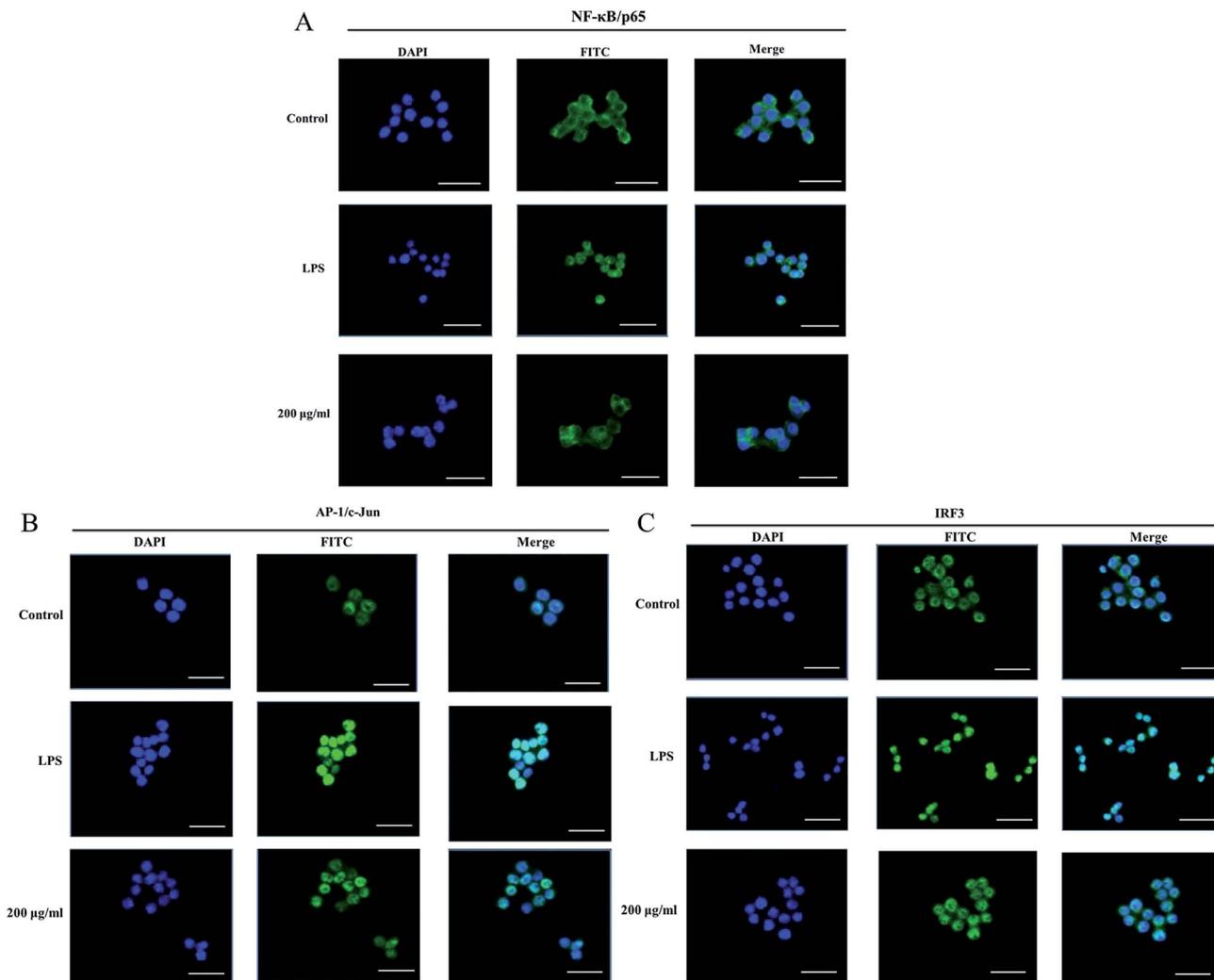
Fig. 7 RIS suppressed the nuclear translocation of NF-κB/p65, AP-1/c-Jun, and IRF3 in the LPS activated RAW 264.7 macrophages cells were incubated with indicated concentrations of RIS for 1 h and then stimulated with LPS for 1 h. The nuclear localization of (A) NF-κB/p65, (B) AP-1/c-Jun, and (C) IRF3 were determined by immunofluorescence staining. The bar in each photograph indicates 33 μm.

carrageenin-induced paw oedema in rats, which may be related to the inhibitory action on the release of inflammatory mediators.[32] Moreover, geniposide also exerted potential anti-inflammatory activity *via* inhibition of the NF-κB signaling pathway.[33] Hence, the suppressive effects of RIS on inflammatory mediators may be, at least in part, due to the presence of these two compounds. Further studies will be conducted to identify other active components responsible for the anti-inflammatory effect of RIS.

Current drug treatment options against inflammation such as NSAID are not satisfactory because of their serious adverse effects and toxicity.[34] Therefore, researchers are seeking new therapeutic agents with high efficacy and safety. In our study, the cell viability was not altered up to 400 μg mL^{-1} of RIS concentration, suggesting that RIS has relatively low toxicity. Moreover, the upregulation of the inflammatory mediators including NO and PGE$_2$ in the RAW 264.7 cells was suppressed by RIS. Previous reports have shown that the excessive production of NO and PGE$_2$ by

macrophages promotes inflammation, immune mediated disorders as well as the symptoms of redness, swelling, and pain.[35,36] Therefore, the inhibition of NO and PGE$_2$ by RIS strongly supports its effectiveness and common use in the treatment of inflammatory diseases. Furthermore, the key enzymes responsible for the synthesis of NO and PGE$_2$ are iNOS and COX-2, respectively.[31,37] In our present study, RIS potentially reduced the LPS induced upregulation of iNOS and COX-2 in the RAW 264.7 cells, showing that the inhibitory effect on the NO and PGE2 production was closely related to the suppression of iNOS and COX-2 expression, respectively.

Several studies have proposed novel strategies for the treatment of inflammatory diseases by regulating the activities of macrophages as well as the levels of cytokines (*e.g.* TNF-α, IL-6, and IL-1β)[38] and chemokines (MCP-1, MIP1-α, and CCL-5).[39] The TLR4 signaling pathway, which regulates the release of pro-inflammatory cytokines and chemokines, is believed to be one of the novel therapeutic
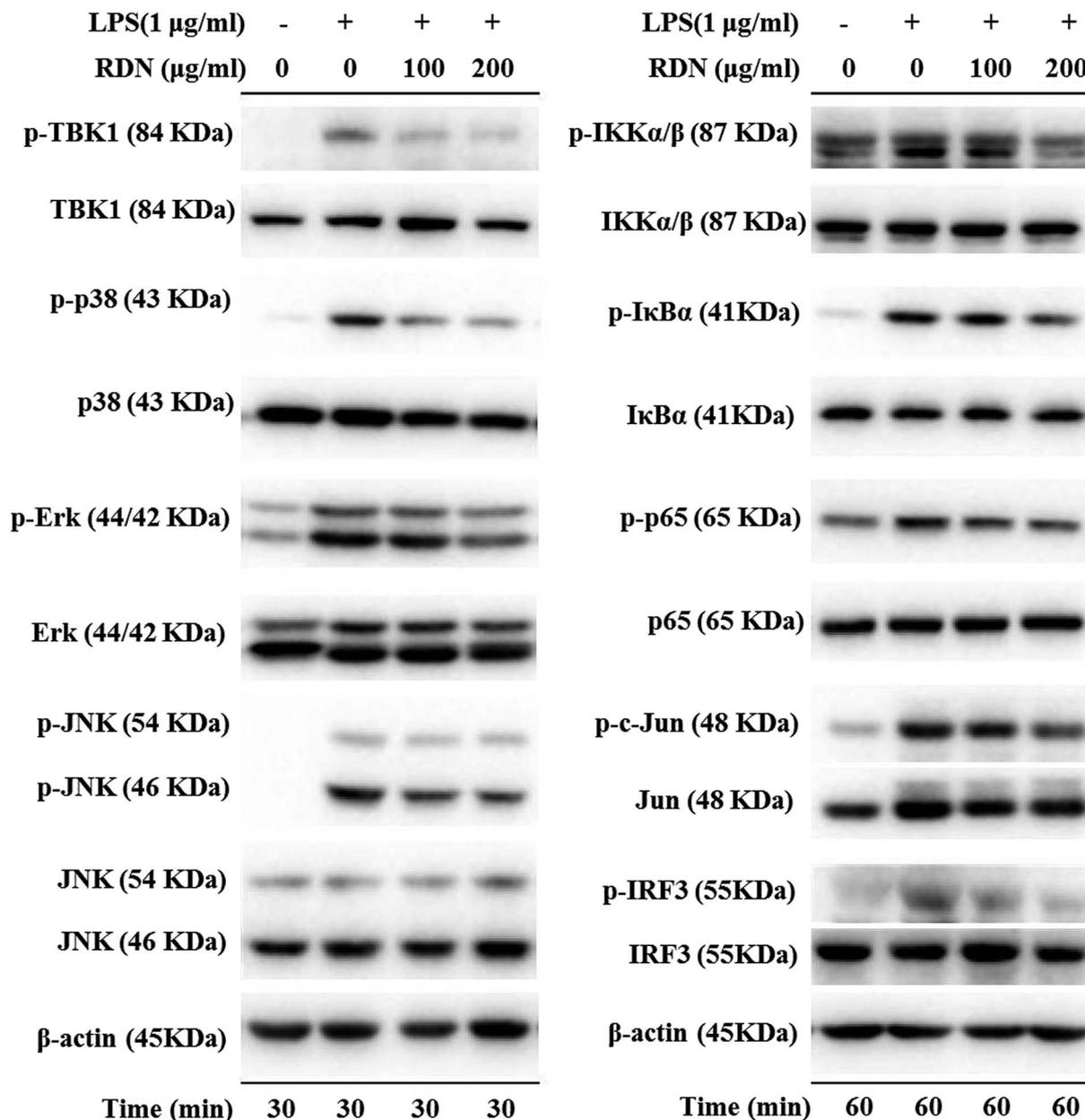
Fig. 8 RIS inhibited IKKα/β/IκBα/NF-κB, MAPKs/AP-1, and TBK1/IRF3 pathways in the LPS activated RAW 264.7 macrophages cells were incubated with indicated concentrations of RIS for 1 h and then stimulated with LPS for 30 min or 60 min. The phosphorylation and total levels of TBK1, IKKα/β, IκBα, NF-κB, p38, ERK, JNK, c-Jun, IRF3, and p65 were detected.

targets in the treatment of inflammatory diseases.[40–42] Our results showed that RIS effectively decreased the over-production of TNF-α, IL-6, IL-1β, MCP-1, MIP1-α, and CCL-5 induced by the LPS-treatment in RAW 264.7 cells, suggesting the inhibitory effect of RIS on inflammatory mediators. This may contribute to its regulative action on the TLR4 signaling transduction.

Upon ligand binding, TLR4 recruits intracellular adapters including MyD88 and activates the IKK complex (including IKKα, IKKβ and IKKγ), which phosphorylates the IκB proteins and lead to its ubiquitination and degradation.[43] Subsequently, the NF-κB/p65 complexes are released from

IκB and translocate from the cytoplasm to the nucleus. This activates the transcription of a variety of genes participating in the immune and inflammatory responses.[44] Our results indicated that RIS significantly reduced the nuclear trans-location and phosphorylation of NF-κB and its upstream kinases including IKKα/β and IκBα in the LPS-treated RAW 264.7 cells, showing that RIS suppressed the IKKα/β/IκBα/NF-κB signaling pathway. MAPKs are mainly composed of three characterized subfamilies, namely, ERK1/2, JNK, and p38 MAPK, which stimulate many cellular functions in physiological conditions and are involved in the pathogenesis of many diseases.[45] In response to LPS stimulation, MAPKs are
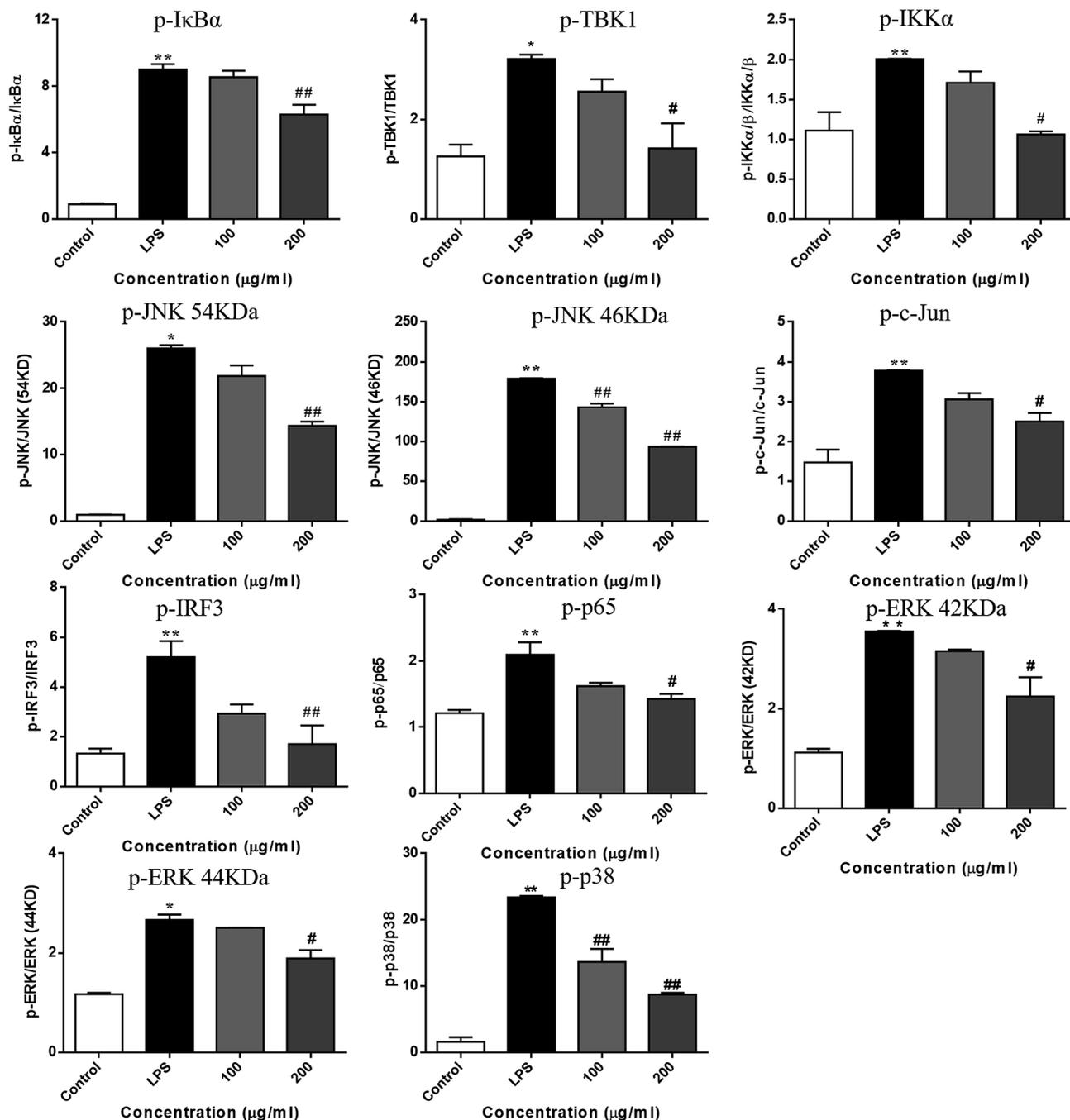
Fig. 9 RIS affected the molecular components of IKKα/β/IκBα/NF-κB, MAPKs/AP-1, and TBK1/IRF3 pathways in the LPS activated RAW 264.7 macrophages cells were incubated with indicated concentrations of RIS for 1 h and then stimulated with LPS for 30 min or 60 min. The phosphorylation and total levels of TBK1, IKKα/β, IκBα, NF-κB, p38, ERK, JNK, c-Jun, IRF3, and p65 were detected. Values are the mean ± SEM of four experiments. **$p < 0.01$ is significantly different from the control. #$p < 0.05$ and ##$p < 0.01$ are different from the LPS alone.

activated through dual phosphorylation of tyrosine and threonine residues, and lead to the activation of AP-1.[46] Our current study suggested that the phosphorylation of MAPKs (ERK1/2, JNK, and p38 MAPK) was suppressed after the RIS treatment. The nuclear translocation and phosphorylation of AP-1 (c-Jun) was also inhibited by the RIS treatment, revealing that RIS inhibited the MAPKs/AP-1 signaling transduction. In addition to the MyD88-dependent pathways,

the TBK1/IRF3 signaling cascade is the main pathway responsible for the induction of type-I interferon production.[47] TBK1 can phosphorylate IRF3 and promotes it nuclear translocation, leading to the expression of IFN-β and CCL-5.[27] Our data represent that the nuclear and phosphorylation levels of IRF3 as well as the phosphorylated TBK1 were decreased by the RIS treatment, indicating that RIS impeded the LPS-induced TBK1/IRF3 axis.
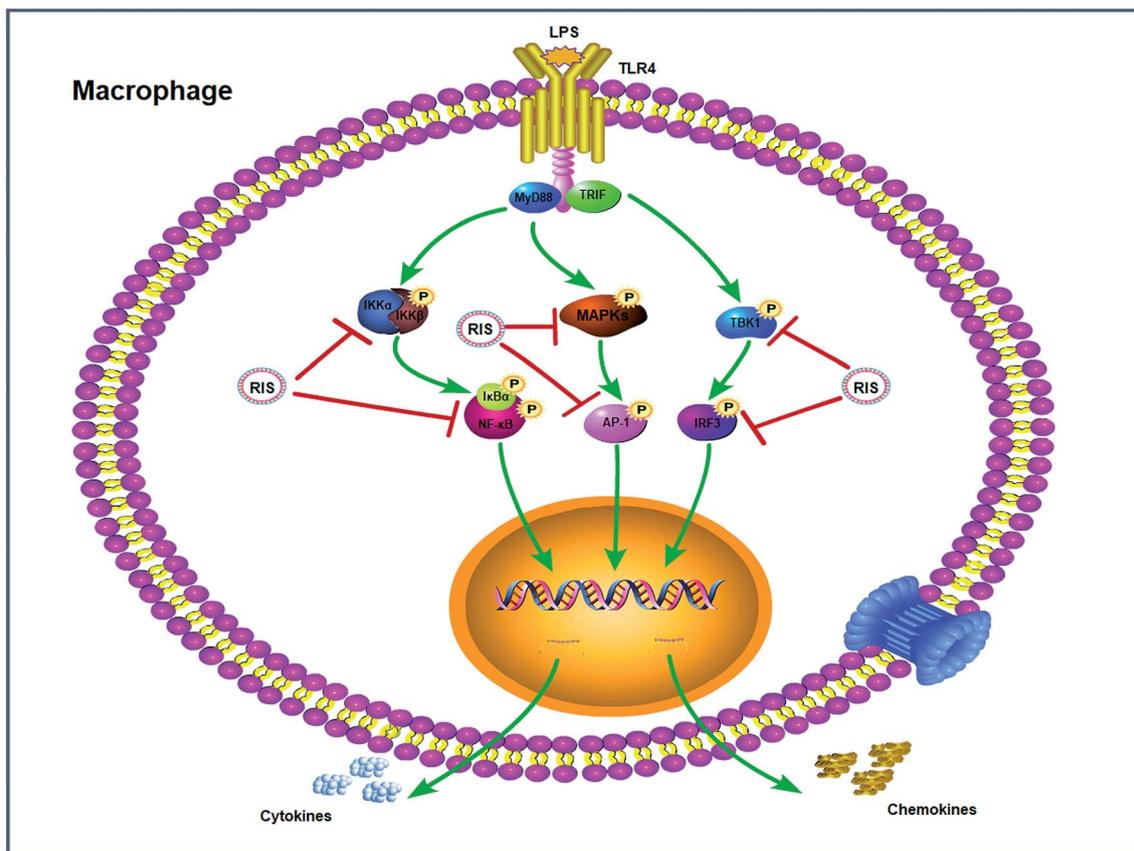
Fig. 10 Inflammatory signaling cascade targeted by RIS in macrophages.

Conclusion

The result demonstrates that the suppressive capabilities of RIS on inflammatory mediators may be attributed to the inhibition of IKKα/β/IκBα/NF-κB, MAPKs/AP-1, and TBK1/IRF3 signaling pathways in the LPS-stimulated RAW 264.7 cells (Fig. 10). To further investigate the contribution of the TLR4 related pathways in the anti-inflammatory effects of RIS, we will establish animal models to validate it.

Chemical compounds studied in this article

Lipopolysaccharide (PubChem CID: 11970143)
Dimethyl sulfoxide (PubChem CID: 679)
Penicillin (PubChem CID: 5904)
Streptomycin (PubChem CID: 19649)

Abbreviations

CCL-5	Chemkine (C–C motif) ligand 5
AP-1	Activator protein-1
DMEM	Dulbecco's modified eagle medium
ERK	Extracellular signal-regulated kinase
FBS	Fetal bovine serum
IKK	IκB kinase
IL	Interleukin
IFN	Interferon
IRF3	IFN regulatory factor 3
JNK	c-Jun N-terminal kinase
LPS	Lipopolysaccharide
MAPK	Mitogen-activated protein kinase
MCP	Monocyte chemoattractant protein
MIP	Macrophage inflammatory protein
MTT	3-(4,5-Dimethylthiazol-2-yl)-2,5-diphenylthiazolium bromide
MyD88	Myeloid differentiation primary response 88
NF-κB	Nuclear factor-κB
p38	p38 mitogen-activated protein kinase
TBK1	TANK-binding kinase 1
TRIF	TIR-domain-containing adaptor protein-inducing IFN-β
TNF	Tumour necrosis factor
TLR	Toll-like receptor
COX-2	Cyclooxygenase-2
iNOS	Inducible nitric oxide synthase

Conflicts of interest

The authors declare no conflicts of interest regarding the publication of this paper.

Acknowledgements

References

1 W. Liao, X.-J. He, Z.-W. Yi, W. Xiang and Y. Ding, *Biomed. Pharmacother.*, 2018, **107**, 1151–1159.

2 I. Sulaiman, L. C. Woei, S. H. Liong and J. Stanslas, *Pulm. Pharmacol. Ther.*, 2016, **40**, 52–68.

3 D. Droemann, S. P. Aries, F. Hansen, M. Moellers, J. Braun, H. A. Katus and K. Dalhoff, *Chest*, 2000, **117**, 1679–1684.

4 J.-G. Chu, X.-J. Wang, H. J. Bi, L.-F. Li, M.-G. Ren and J.-W. Wang, *Int. Immunopharmacol.*, 2018, **59**, 174–180.

5 Z. Vitenberga, M. Pilmane and A. Babjoniševa, *Pathol., Res. Pract.*, 2019, **215**, 97–105.

6 H.-B. Guo and M.-X. Chen, *Ecotoxicol. Environ. Saf.*, 2018, **161**, 184–189.

7 India State-Level Disease Burden Initiative CRD Collaborators, *Lancet Global Health*, 2018, **6**, 1363–1374.

8 E. Midouhas, E. Flouri, E. Papachristou and T. Kokosi, *Intelligence*, 2018, **68**, 30–36.

9 C. Li, Q. Liu and L.-Q. Xie, *Biochem. Biophys. Res. Commun.*, 2018, **507**, 22–29.

10 X.-C. Zheng, D. Yang, X. Liu, N. Wang, B. Li, H.-W. Cao, Y.-L. Lu, G. Wei, H. Zhou and J. Zheng, *Int. Immunopharmacol.*, 2010, **10**, 1209–1219.

11 F. Liu, Y. Wen, J.-Y. Kang, C.-Y. Wei, M.-H. Wang, Z.-Q. Zheng and J.-T. Peng, *Int. J. Mol. Med.*, 2018, **42**, 1436–1444.

12 A. A. Shalmani, M. H. Ghahremani, F. Jeivad, A. Shadboorestan, G. Hassanzadeh, A. Beh-Pajooh, M. Ganbari-Erdi, S. Kasirzadeh, M. Mojtahedzadeh and O. Sabzevari, *Life Sci.*, 2018, **215**, 152–158.

13 M. Zhang, J. Wu, J. Han, H. Shu and K. Liu, *Chem. Cent. J.*, 2018, **12**, 109.

14 W.-X. Ding, J.-Y. Gu, L. Cao, N. Li, G. Ding, Z.-Z. Wang, L.-R. Chen, X.-J. Xu and W. Xiao, *J. Ethnopharmacol.*, 2014, **155**, 589–598.

15 B. C.-Y. Cheng, X.-Q. Ma, H. Y. Kwan, K. W. Tse, H.-H. Cao, T. Su, X. Shu, Z.-Z. Wu and Z.-L. Yu, *J. Ethnopharmacol.*, 2014, **153**, 922–927.

16 Y.-Z. He, *Chinese Medicine Modern Distance Education of China*, 2015, **9**, 123–125.

17 China Food and Drug Administration, *National drug standards of Re-Du-Ning injection: YBZ08202005-2015Z*, 2015, pp. 1–8.

18 T.-F. Tzeng, Y.-C. Tzeng, Y.-J. Cheng, S.-S. Liou and I.-M. Liu, *Nutrients*, 2015, **7**, 8670–8684.

19 Y.-J. Lin, C.-C. Lai, C.-H. Lai, S.-C. Sue, C.-W. Lin, C.-H. Hung, T.-H. Lin, W.-Y. Hsu, S.-M. Huang, Y.-L. Hung, N. Tien, X. Liu, C.-L. Chen and F.-J. Tsai, *Eur. J. Med. Chem.*, 2013, **62**, 206–213.

20 E. Hsu, *Trans. R. Soc. Trop. Med. Hyg.*, 2006, **100**, 505–508.

21 F. V. D. Kooy and S. E. Sullivan, *J. Ethnopharmacol.*, 2013, **150**, 1–13.

22 S. H. Park, E. Roh, H. S. Kim, S. I. Baek, N. S. Choi, N. Kim, B. Y. Hwang, S. B. Han and Y. Kim, *Biochem. Biophys. Res. Commun.*, 2013, **442**, 183–188.

23 S.-J. Kim, S.-J. Yoon, Y.-M. Kim, S.-W. Hong, S. H. Yeon, K.-I. Choe and S.-M. Lee, *J. Ethnopharmacol.*, 2014, **155**, 256–266.

24 Q.-H. Shi, J.-J. Cao, L. Fang, H.-Y. Zhao, Z.-X. Liu, J.-H. Ran, X.-C. Zheng, X.-L. Li, Y. Zhou, D. Ge, H.-M. Zhang, L. Wang, Y. Ran and J.-F. Fu, *Int. Immunopharmacol.*, 2014, **20**, 298–306.

25 K. H. Park, Y. D. Yoon, S.-B. Han, S. J. Oh, J. Yun, C. W. lee, K. Lee, S.-K. Park, H. M. Kim and J. S. Kang, *Int. Immunopharmacol.*, 2012, **14**, 580–584.

26 Y. Zhang, H. Guo, B. C.-Y. Cheng, T. Su, X.-Q. Fu, T. Li, P.-L. Zhu, K.-W. Tse, S.-Y. Pan and Z.-L. Yu, *Drug Des., Dev. Ther.*, 2018, **12**, 2731–2748.

27 G. Luo, B. Cheng, H. Zhao, X.-Q. Fu, R. Xie, S.-F. Zhang, S.-Y. Pan and Y. Zhang, *Molecules*, 2018, **23**, 3319.

28 H.-T. Shi, L. Dong, X.-Y. Dang, Y.-P. Liu, J. Jiang, Y. Wang, X.-L. Lu and X.-Y. Guo, *Inflammation Res.*, 2013, **62**, 581–587.

29 A.-Y. Kim, H.-J. Shim, S. Y. Kim, S. Heo and H.-S. Youn, *Int. Immunopharmacol.*, 2018, **64**, 1–9.

30 J. Liu, K. Sun, C. Zheng, X. Chen, W. Zhang, Z. Wang, P. A. Shar, W. Xiao and Y. Wang, *PLoS One*, 2015, **10**, e0123109.

31 S. J. Hwang, Y.-W. Kim, Y. Park, H. J. Lee and K.-W. Kim, *Inflammation Res.*, 2014, **63**, 81–90.

32 M. D. d. Santos, M. C. Almeida, N. P. Lopes and G. E. P. d. Souza, *Biol. Pharm. Bull.*, 2006, **29**, 2236–2240.

33 R. Deng, F. Li, H. Wu, W.-Y. Wang, L. Dai, Z.-R. Zhang and J. Fu, *Front. Pharmacol.*, 2018, **9**, 105.

34 J. R. Perkins, M. Sanak and G. Canto, *Trends Pharmacol. Sci.*, 2015, **36**, 172–180.

35 X.-H. Jin, K. Ohgami, K. Shiratori, Y. Suzuki, Y. Koyama, K. Yoshida, I. Ilieva, T. Tanaka, K. Onoe and S. Ohno, *Exp. Eye Res.*, 2006, **82**, 860–867.

36 R. M. Hinson, J. A. Williams and E. Shacter, *Proc. Natl. Acad. Sci. U. S. A.*, 1996, **93**, 4885–4890.

37 J. Y. Park, M. H. Pillinger and S. B. Abramson, *Clin. Immunol.*, 2006, **119**, 229–240.

38 T.-T. Zhang, T. Hu, J.-G. Jiang, J.-W. Zhao and W. Zhu, *RSC Adv.*, 2018, **8**, 7134–7141.

39 P. M. Murphy, Chemokines and Chemokine Receptors, *Clinical Immunology*, ed. R. R.Rich, T. A.Fleisher, W. T.Shearer, H. W.Schroeder, A. J.Frew and C. M.Weyand, Content Repository Only!, London, 5th edn, 2019, vol. 10, pp. 157–170.

40 T. Baluchnejadmojarad, Z. Kiasalari, S. A. Majd, Z. Ghasemi and M. Roghani, *Eur. J. Pharmacol.*, 2017, **794**, 69–76.

41 L.-H. Xu, Y.-B. Liu, Y.-H. Sun, H. Li, W.-D. Mi and Y.-G. Jiang, *Biomed. Pharmacother.*, 2018, **107**, 526–533.

42 H. Capiralla, V. Vingtdeux, H.-T. Zhao, R. Sankowski, Y. A. Abed, P. Davies and P. Marambaud, *J. Neurochem.*, 2012, **120**, 461–472.

43 S. Akia and K. Takeda, *Nat. Rev. Immunol.*, 2004, **4**, 499.

44 G. M. Barton and R. Medzhitov, *Science*, 2003, **300**, 1524.

45 Q.-H. Shao, X.-L. Zhang, Y. Chen, C.-G. Zhu, J.-G. Shi, Y.-H. Yuan and N.-H. Chen, *Mol. Immunol.*, 2018, **99**, 115–123.

46 T. Kawasaki and T. Kawai, *Front. Immunol.*, 2014, **5**, 461.

47 S. Wei, D.-B. Yang, J.-F. Yang, X.-S. Zhang, J.-L. Zhang, J.-C. Fu, G.-B. Zhou, H.-J. Liu, Z.-X. Lian and H.-B. Han, *Eur. J. Cell Biol.*, 2019, **98**, 36–50.